THE UNIVERSITY of EDINBURGH

Edinburgh Research Explorer

Multiple spatial behaviours govern social network positions in a wild ungulate

OPEN ACCESS

Multiple spatial behaviours govern social network positions in a wild ungulate

Gregory F Albery[1,2*], Alison Morris[2], Sean Morris[2], Josephine M Pemberton[2], Tim H. Clutton-Brock[2,3], Daniel H Nussey[2], Josh A Firth[4,5]

1. Department of Biology, Georgetown University, Washington, DC
2. Institute of Evolutionary Biology, University of Edinburgh, Edinburgh, UK
3. Department of Zoology, University of Cambridge, Cambridge, UK
4. Department of Zoology, University of Oxford, Oxford, UK
5. Merton College, University of Oxford, Oxford, UK

*gfalbery@gmail.com

Abstract

The structure of wild animal social systems depends on a complex combination of intrinsic and extrinsic drivers. Population structuring and spatial behaviour are key determinants of individuals' observed social behaviour, but quantifying these spatial components alongside multiple other drivers remains difficult due to data scarcity and analytical complexity. We used a 43-year dataset detailing a wild red deer population to investigate how individuals' spatial behaviours drive social network positioning, while simultaneously assessing other potential contributing factors. Using Integrated Nested Laplace Approximation (INLA) multi-matrix animal models, we demonstrate that social network positions are shaped by two-dimensional landscape locations, pairwise space sharing, individual range size, and spatial and temporal variation in population density, alongside smaller but detectable impacts of a selection of individual-level phenotypic traits. These results indicate strong, multifaceted spatiotemporal structuring in this society, emphasising the importance of considering multiple spatial components when investigating the causes and consequences of sociality.

Word Count: **Abstract**: 143 words; **Main text**: 4720 words
Number of figures: 4; Number of tables: 0; Number of references: 53

Authorship Statement

Data Accessibility Statement
The code used here is available at https://github.com/gfalbery/Spocial_Deer. On acceptance, the data will be uploaded to the same repo, which will be archived on Zenodo.

Introduction

Social behaviour is an integral component of an animal's phenotype, driving processes including disease transmission, mating, learning, and selection (Croft *et al.* 2008; VanderWaal *et al.* 2014; Krause *et al.* 2015; Firth *et al.* 2018; Sah *et al.* 2018; Silk *et al.* 2019; Firth 2020). Contemporary studies of animal behaviour often use social networks to derive individual-level network positions, under the assumption that between-individual variation in network positioning is indicative of between-individual variation in social behaviour (Franks *et al.* 2010; Krause *et al.* 2015; Sosa *et al.* 2020). However, an animal's position in its social network also interacts with its own spatial behaviour (Pinter-Wollman *et al.* 2014; Spiegel *et al.* 2016; Webber & Vander Wal 2018; Albery *et al.* 2020a), and with a range of extrinsic factors: demography determines local population density and structuring (Shizuka & Johnson 2019)**,** while the environment shapes resource distributions, movement corridors, and emergent patterns of space use, all of which will influence the architecture of the social system (Firth & Sheldon 2016; Webber & Vander Wal 2018; Farine & Sheldon 2019; He *et al.* 2019). Moreover, the social environment itself can drive space use decisions, creating a bidirectional causal relationship between the two (Firth & Sheldon 2016; Spiegel *et al.* 2016). As such, it is important to consider spatial behaviour and environmental context when assessing the causes and consequences of individual-level social network positioning (Pinter-Wollman *et al.* 2014; Spiegel *et al.* 2016; Webber & Vander Wal 2018; He *et al.* 2019; Albery *et al.* 2020a), yet doing so remains difficult in most systems due to the complexity of spatial-social analyses that incorporate these processes.

The spatial correlates of social network structure are poorly understood because they are highly multivariate and (therefore) difficult to analyse. Encouragingly, strong support exists for simple associations between individuals' spatial and social behaviours. For example, spatial proximity and social connections are often correlated, because 1) individuals that share more space are more likely to associate or interact and 2) those that are socially affiliated are likely to opt to share more space (Firth & Sheldon 2016; Spiegel *et al.* 2016). Correlated spatial-social proximity has been observed in diverse taxa including elk (Vander Wal *et al.* 2014), raccoons (Robert *et al.* 2012), birds (Firth & Sheldon 2016), and myriad other systems. Similarly, spatial and social network centrality are occasionally found to correlate (Mourier *et al.* 2019), as are temporal variation in population density and social contact rates (Sanchez & Hudgens 2015). However, spatial behaviours can be summarised using a wide range of metrics, including individuals' spatial activity levels (e.g. home range area), pairwise space sharing (e.g. distances or home range overlaps), demographic structure (e.g. temporal population size or local conspecific density), and point location on the two-dimensional landscape; the interplay between these spatial traits and social network

70   positioning are much more poorly understood than spatial-social proximity. For example, are
71   more social individuals simply wider-ranging, leading them to make more contacts? Do they
72   most often inhabit areas of high population density or well-used movement corridors? These
73   variable spatial components take a combination of different data structures, and are
74   therefore difficult to include in the same models, particularly in large numbers and alongside
75   a range of other individual-level phenotypes. Additionally, spatial data such as telemetry or
76   "gambit of the group" approaches are occasionally used to approximate or estimate social
77   behaviour, so space and sociality may be confounded at the data collection level, and may
78   then be difficult to extricate (Albery *et al.* 2020a). It is therefore unclear to what extent
79   individuals' social network positions are representative of 1) their own social behaviour; 2)
80   their own spatial behaviour; 3) their situation within the population; 4) other aspects of their
81   biotic and abiotic environment such as landscape structure; and 5) the intrinsic phenotypic
82   traits that researchers are commonly interested in investigating.

83   Several frameworks have been proposed to facilitate the untangling of spatial and social
84   processes in wild animals (Jacoby & Freeman 2016; Silk *et al.* 2018, 2019; Webber &
85   Vander Wal 2018; Mourier *et al.* 2019; Albery *et al.* 2020a). To date, statistical methods
86   focus on incorporating socio-spatial behaviours into the node-and-edge structure of network
87   data, using e.g. null network permutations (Firth & Sheldon 2016), spatially embedded
88   networks (Daraganova *et al.* 2012), and nested "networks of networks" composed of
89   movement trajectories (Mourier *et al.* 2019). Many such analyses involve reducing
90   movement patterns into some form of spatial network based on home range overlap or
91   spatial proximity between dyads, which are then incorporated into models. For example,
92   statistical models named "animal models" can examine spatial variation by fitting such
93   matrices as variance components, potentially alongside other dyadic similarity matrices (i.e.,
94   pairwise measures of similarity), to quantify genetic and non-genetic contributions to
95   individuals' phenotypes (Kruuk 2004; Stopher *et al.* 2012b; Regan *et al.* 2016; Thomson *et*
96   *al.* 2018; Webber & Vander Wal 2018). As yet, the focus on controlling for spatial
97   autocorrelation using space sharing and network permutations has contributed to a lack of
98   clarity concerning the role that spatial behaviour and environmental context play in driving
99   social network positioning (Albery *et al.* 2020a).

100   Studies across ecological disciplines increasingly use Integrated Nested Laplace
101   Approximation (INLA) models to control for spatial autocorrelation in a multitude of contexts
102   (Lindgren *et al.* 2011; Lindgren & Rue 2015; Zuur *et al.* 2017). As well as including fixed and
103   random effects to quantify individual-level drivers, these models can incorporate dyadic
104   space sharing components (Holand *et al.* 2013) and stochastic partial differentiation
105   equation (SPDE) effects to model 2-dimensional spatial patterns in the response variable,

106   thereby controlling for and estimating spatiotemporal variation associated with fine-scale

107   positioning within the landscape (Albery *et al.* 2019). As such, these models offer an exciting

108   opportunity to test and compare the roles of a range of spatial behaviours and

109   autocorrelation structures, alongside phenotypic drivers, in determining social network

110   positioning.

111   We address this question using the long-term study in the Isle of Rum red deer (*Cervus*

112   *elaphus*). These study animals comprise an unmanaged wild population with a contiguous

113   fission-fusion social system (Clutton-Brock *et al.* 1982). They experience strong

114   environmental gradients and (therefore) exhibit spatial autocorrelation in a number of

115   important phenotypes: individuals with greater home range overlap have more similar

116   behavioural and life history traits (Stopher *et al.* 2012b), and those in closer proximity have

117   more similar parasite burdens (Albery *et al.* 2019). Further, as with other matrilineal

118   mammalian systems, closely related individuals frequently associate (Clutton-Brock *et al.*

119   1982) and live closer together (Stopher *et al.* 2012b). Individuals have highly repeatable

120   home ranges (Stopher *et al.* 2012b) that decline in size over their lifetimes, predicting

121   declining survival probability (Froy *et al.* 2018). The study area has a strong spatial gradient

122   in resource availability, with high-quality grazing heavily concentrated in the far north of the

123   system, and with most individuals aggregating around this area (Mcloughlin *et al.* 2006),

124   such that population density decreases outwards towards the edge of the study population

125   (Clutton-Brock *et al.* 1982). As such, the deer comprise a useful system for assessing

126   spatial-social relationships in the wild.

127   To assess how individuals' spatial behaviours translate to social network positions, we

128   constructed fine-scale social networks from 43 years of censuses of the study population.

129   We derived 8 different individual-level network positioning measures of varying complexity

130   that are important to different social processes (Krause *et al.* 2015). Using multi-matrix

131   animal models in INLA, we examined whether spatial locations, space sharing, home range

132   area, and local population density explained variation in network position metrics, alongside

133   a range of individual-, temporal-, and population-level factors. Specifically, we aimed to test

134   two hypotheses: that the structure of the social network would be highly dependent on the

135   distribution of population density in space; and that individuals' social network centrality

136   would be largely explained by their ranging behaviour, where wide-ranging individuals were

137   more likely to be socially well-connected. We further expected that space sharing and point

138   locations would uncover substantial spatial autocorrelation in social network positioning, and

139   that different social network metrics would exhibit different spatial patterns and vary drivers.

140   This not only comprises a large-scale empirical examination of the factors shaping social

141   network positions in this extensively monitored wild mammal, but also provides a

142 methodological advancement in developing powerful, flexible new methods (INLA-based
143 multi-matrix animal models) with broad potential for examining spatial-social processes in
144 this and other systems.

Methods

Study system and censusing

147 The study was carried out on an unpredated long-term study population of red deer on the
148 Isle of Rum, Scotland (57°N,6°20′W). The natural history of this matrilineal mammalian
149 system has been studied extensively (Clutton-Brock et al. 1982), and we focussed on
150 females aged 3+ years, as these individuals have the most complete associated census
151 data, and few males live in the study area except during the mating period. Individuals are
152 monitored from birth, providing substantial life history and behavioural data, and >90% of
153 calves are caught and tagged, with tissue samples taken (Clutton-Brock *et al.* 1982). The
154 population thus has comprehensive genomic data, allowing high-powered quantitative
155 genetic analyses: most individuals born since 1982 have been genotyped at >37,000 SNPs,
156 distributed throughout the genome (e.g. Huisman, Kruuk, Ellis, Clutton-Brock, & Pemberton,
157 2016). Census data were collected for the years 1974-2017, totalling 423,070 census
158 observations. Deer were censused by field workers five times a month, for eight months of
159 the year, along one of two alternating routes (Clutton-Brock *et al.* 1982). Individuals'
160 identities, locations (to the nearest 100M), and group membership were recorded. Grouping
161 events were estimated by seasoned field workers according to a variant of the "chain rule"
162 (e.g. Castles et al., 2014), where individuals grazing in a contiguous group within close
163 proximity of each other (each individual under ~10 metres of at least one other individual in
164 the group) were deemed to be associating, with mean 130.4 groups observed per individual
165 across their lifetime (range 6-943). The mortality period falls between Jan-March, when there
166 is least available food, and minimal mortality occurs outside this period. We only used
167 census records in each May-December period, from which we derived annual social network
168 position measures as response variables (Figure 1-2). We elected to investigate this
169 seasonal period because it stretches from the spring calving period until the beginning of the
170 mortality period, simplifying network construction and avoiding complications arising from
171 mortality events. Our dataset totalled 3356 annual observations among 532 grown females
172 (Figure 1).

173 In this system, female reproduction imposes substantial costs for immunity and parasitism
174 (Albery *et al.* 2020c), and for subsequent survival and reproduction (Clutton-Brock, Albon, &
175 Guinness, 1989; Froy, Walling, Pemberton, Clutton-Brock, & Kruuk, 2016). If a female
176 reproduces, she produces 1 calf per year in the spring, generally beginning in May; the "deer

177 year" begins on May 1 for this reason. Here, reproductive status was classified into the

178 following four categories using behavioural observations: True Yeld (did not give birth);

179 Summer Yeld (the female's calf died in the summer, before 1st October); Winter Yeld (the

180 female's calf died in the winter, after 1st October); and Milk (calf survived to 1st May the

181 following calendar year).

Generating spatial and social matrices

183 All code is available online at https://github.com/gfalbery/Spocial_Deer. We constructed the

184 home range overlap (HRO) matrix using the R package AdeHabitatHR (Calenge 2011),

185 following previous methodology (Stopher *et al.* 2012b; Regan *et al.* 2016; Froy *et al.* 2018).

186 First, using a kernel density estimation method, we derived lifetime home ranges for each

187 individual with more than five census observations. Previous analysis has shown that this

188 system is robust to the number of observations used to generate home ranges (Froy *et al.*

189 2018). We used lifetime home ranges to fit one value per individual in the animal models;

190 individual ranges (and range sizes) correlate strongly from year to year (Stopher *et al.*

191 2012b; Froy *et al.* 2018). We derived proportional HRO of each dyad using Bhattacharya

192 Affinity (following Stopher *et al.* 2012b), producing values between 0-1 (i.e. no overlap to

193 complete overlap).

194 To control for individuals' two-dimensional point locations, we used a Stochastic Partial

195 Differentiation Equation (SPDE) effect in INLA. This effect models the distance between

196 points to calculate spatial autocorrelation, using Matern covariance (Lindgren *et al.* 2011).

197 This random effect used individuals' annual centroids (mean easting and northing in a given

198 year) or lifetime centroids (mean easting and northing across all observations) as point

199 locations to approximate spatial variation in the response variable (Lindgren *et al.* 2011;

200 Albery *et al.* 2019).

201 We used a genomic relatedness matrix (GRM) using homozygosity at 37,000 Single

202 Nucleotide Polymorphisms, scaled at the population level (Yang *et al.* 2011; for a population-

203 specific summary, see Huisman *et al.* 2016). This matrix is well-correlated with pedigree-

204 derived relatedness metrics (Huisman *et al.* 2016). HRO was well-correlated with distance

205 between lifetime centroids (i.e., closer individuals tended to share more range), and both

206 were weakly but significantly correlated with genetic relatedness (Supplementary Figure 1).

207 To test whether social network positions could be explained by population density, we

208 derived the local density of individuals again using AdeHabitatHR (Calenge 2011). We

209 generated density kernels of observations, and then assigned individual deer their local

210 population density based on their location on this kernel, following previous methodology

211 developed in badgers (Albery *et al.* 2020b). This local density value was then fitted as a fixed

212   explanatory variable. We used four different density metrics, each examining the density of a

213   different observation type: lifetime centroids ("lifetime density"); annual centroids ("annual

214   density"); all observations across the study period ("sighting density"); and all observations in

215   the focal year ("annual sighting density"). Only one such density metric was fitted at once.

216   We also calculated annual home range areas (HRA) by taking the 70% isopleth of each

217   individual's annual space use distribution, following previous methodology (Froy *et al.* 2018).

218   This HRA variable was fitted as a fixed effect in the same way as local density.

219   We constructed a series of 43 annual social networks using "gambit of the group," where

220   individuals in the same grouping event (as described above) were taken to be associating

221   (Franks *et al.* 2010). Dyadic associations were calculated using the simple ratio index

222   (Cairns & Schwager 1987) derived as a proportion of total sightings (grouping events) in

223   which the focal individuals were seen together: $Sightings_{A,B}/(Sightings_A+Sightings_B-$

224   $Sightings_{A,B})$, or $Intersect_{A,B}/Union_{A,B}$. In this dyadic matrix, 0=never seen together and

225   1=never seen apart.

Statistical Analysis

227   ***Metrics.*** Using the annual social networks, we derived eight individual-level network metrics

228   which are commonly used across animal social networks and have been considered in

229   detail(Whitehead 2008; Brent 2015; Krause *et al.* 2015; Firth *et al.* 2017). We set each of

230   these network metrics for use as response variables in separate INLA Generalised Linear

231   Mixed Models (GLMMs) with a Gaussian family specification. In increasing order of

232   complexity, our measures included four direct sociality metrics, which only take into account

233   an individual's connections with other individuals: 1) Group Size – the average number of

234   individuals a deer associated with per sighting; 2) Degree – the number of unique individuals

235   she was observed with; 3) Strength – sum of all their weighted social associations to others;

236   4) Mean Strength – an individual's average association strength to each of the unique

237   individuals she was observed with (equivalent to strength divided by degree). We also

238   included four more complex "indirect" metrics (all using algorithms as specified from (Csardi

239   & Nepusz 2006)), which also take into account an individual's connections' connections: 5)

240   Eigenvector centrality – which considers the sum of their own connections and the sum of

241   their associates' connections; 6) Weighted Eigenvector – which is akin to eigenvector

242   centrality but also accounts for the weights of theirs, and their associates, connections; 7)

243   Betweenness – the number of shortest paths that pass through the focal individual to

244   traverse the whole network; 8) Clustering (local) – the tendency for an individual's contacts

245   to be connected to one another, forming triads. The raw, untransformed correlations were

246   assessed for all metrics, and R lay between -0.5 and 0.879 across metrics (Supplementary

247   Figure 2). When modelling them as response variables, to approximate normality, all social

248   metrics were square root-transformed apart from eigenvector centralities (which were left

249   untransformed), group size (which was cube root-transformed), and betweenness (which

250   was log(X+1)-transformed). Each social network metric was fitted as a response variable in

251   a separate model set (as outlined conceptually in Figure 1).

252   **Base model structure.** We ensured that all models followed the same base structure.

253   Random effects included individual identity and year (categorical random intercepts), and the

254   genetic relatedness matrix. Fixed effects included Age (continuous, in years), Reproductive

255   Status (four categories: True Yeld; Summer Yeld; Winter Yeld; and Milk), and Number of

256   observations (continuous, log-transformed to approximate normality), alongside year-level

257   continuous factors including Year (continuous) and annual study Population Size (log-

258   transformed). All continuous response and explanatory variables were standardised to have

259   a mean of zero and a standard deviation of 1. Fixed effect estimates were provided by the

260   mean and 95% credibility intervals of the posterior estimate distribution.

261   **Adding spatial components.** To investigate the divergent value of different spatial

262   behaviours, we iteratively added spatial effects to the base model, investigating which

263   behaviours best fit the data. These spatial behaviours corresponded to four broad

264   components in Figure 1: space sharing (HRO matrix); home range area (HRA); point

265   locations (SPDE effect); and local population density (density fixed effect). For space

266   sharing, we only used one metric: lifetime HRO (see above). For point locations, we selected

267   between 1) lifetime centroids; 2) annual centroids; and 3) annual centroids with a

268   spatiotemporally varying annual field. For density, we used the four metrics outlined above

269   ("lifetime", "annual", "sighting", and "annual sighting" density). To distinguish between

270   competitive models we used Deviance Information Criterion (DIC). In each round, we added

271   each spatial behaviour individually and then kept the best-fitting one, until all four had been

272   added or their addition did not improve the model, using a cutoff of 2 DIC.

273   **Comparing all spatial and non-spatial drivers.** To compare the relative importance of all

274   fixed and random effects, we examined the model's predicted values and their correlations

275   with the observed values, representing the proportion of the variance that was explained by

276   the model (i.e., R^2). We used the model to predict each social behaviour metric, and

277   iteratively held each explanatory variable's predictions at the mean, one at a time. We then

278   assessed the squared correlations of these values with the observed values, relative to

279   those of the full model. Variables with greater effects in the model produced less accurate

280   predicted values when held constant.

Results

Spatial behaviours were important in determining all eight individual-level social network position variables. The non-spatial model was far the poorest-fitting for all eight metrics, and the DIC changes associated with adding spatial components were substantial (Figure 3A). Generally, wide-ranging individuals and those living in areas of greater population density tended to be more central, and space sharing and point location effects both revealed substantial spatial autocorrelation (Figure 3).

Notably, point location-based SPDE effects improved model fit substantially in addition to HRA and density effects, and had a greater effect on model fit than space sharing HRO effects, even when conceptualised at the same timescale (i.e., across the individual's lifetime). Investigating the R^2 components of the models containing only HRO (i.e., without SPDE effects) revealed that in general spatial overlap accounted for more variation than the genetic matrix (Supplementary Figure 3), but comparing these with the other models revealed that the point location effects contributed more than either of these matrices (Figure 3B). Annually varying centroids further improved model fit, and allowing the spatial field to vary between years in our spatiotemporal models improved models even more (Figure 3A). Although the space sharing and genomic relatedness matrices had similar sized impacts on the full models (Figure 3B), removing the SPDE effect resulted in a substantial increase in the HRO effect, but with very little impact on the Genomic Relatedness Matrix's R^2 (Supplementary Figure 3). These findings were relatively consistent across all metrics (Figure 3A-B), although the SPDE effect was notably smaller for betweenness (Figure 3B). Taken together, these results reveal that lifetime space sharing was good at accounting for variation in social behaviour, but that its effect was surpassed by increasingly complex temporal formulations of point location effects.

We compared the importance of all fixed and random effects by predicting selectively from the model, revealing overwhelmingly strong effects of spatiotemporal drivers (Figure 3B). Our models fit well and explained a substantial amount of variation in social network centrality (>70%); the majority of the fit was lent by a combination of the INLA SPDE effect, fixed effects of local population density, and random effects of year (Figure 3B). Space sharing (HRO) and home range area (HRA) had comparatively small effects.

Number of observations also had a notable impact for Degree, Betweenness, and Clustering (Figure 3B). Fixed effects for year and observation numbers were generally strong and significantly positive across metrics, except in the case of clustering, for which observation number's effect was significantly negative (Figure 3B). There were also small positive effects of population size on betweenness and degree centrality (Figure 3B).

316   Although individual-level drivers (reproduction, age, and individual identity) had a negligible

317   impact on all variables' R^2 (Figure 3B), many had a significant effect (i.e., their 95%

318   credibility intervals did not overlap with zero; Figure 3C). Individuals whose calves lived to

319   the winter and then either died before the 1st May ("Winter Yeld") or survived ("Milk") were

320   generally less central than those that did not give birth ("True Yeld") or whose calf died

321   before 1st October ("Summer Yeld"). Similarly, there were minor age-related decreases in

322   network centrality for the direct metrics (Group Size, Degree, and Strength; Figure 3C).

323   To investigate spatial patterns of sociality when accounting for our fixed and random effects,

324   we projected the annual SPDE random effect in two-dimensional space (Figure 4;

325   Supplementary Figures 5-12). The spatial distributions of network centrality metrics were

326   highly variable, but direct metrics generally peaked in the centre of the study system and

327   decreased outwards (Figure 4). Mean Strength was an exception, being lowest in the centre

328   and increasing outward (Figure 4D); Clustering was patchily distributed, such that no clear

329   pattern was evident (Figure 4H); and Betweenness was slightly offset, being highest in the

330   north-northeast of the study area rather than in the central north (Figure 4G). The range of

331   autocorrelation also varied among metrics; Betweenness and Clustering had notably shorter

332   ranges than the other metrics, showing that they change more rapidly in space

333   (Supplementary Figure 4). We also plotted the spatial fields through time, revealing

334   substantial variation in the spatial fields across the study period (Supplementary Figures 5-

335   12).

Discussion

The role of spatial behaviour in driving social network structure

338   The position individuals occupy within their social networks can affect many aspects of their

339   ecology and evolution (Krause *et al.* 2015; Firth *et al.* 2018; Sah *et al.* 2018), and our results

340   confirm the powerful role of fine-scale spatial context in shaping such traits (e.g. Farine &

341   Sheldon, 2019; Mourier et al., 2019; Webber & Vander Wal, 2018). Capitalising on our

342   models' ability to compare the influence of a wide range of spatial and non-spatial

343   components, we found that spatial behaviour and environmental context were the most

344   important correlates of social network centrality -- more so than a suite of individual-level

345   phenotypes and demographic factors. Individuals with larger ranges and inhabiting higher-

346   density areas were more central in the social network, revealing the important role of

347   individual spatial activity levels and location within the broader population structure. As

348   expected, models were further improved when we incorporated pairwise space sharing and

349   two-dimensional point locations, demonstrating that an individual's social network position is

350   not determined simply by the density of nearby individuals and by its own spatial activity, but

351 by other aspects of the fine-scale surrounding environment such as microclimate, resource
352 distribution, and landscape architecture (Spiegel *et al.* 2018; Webber & Vander Wal 2018;
353 He *et al.* 2019). Reciprocally, individuals may be altering their spatial behaviour, e.g. opting
354 to share more space or live closer together if they are more socially connected (Firth &
355 Sheldon 2016; Spiegel *et al.* 2016). As such, we propose that social network studies should
356 more regularly incorporate both space sharing and (temporally varying) point locations in
357 their statistical approaches to anticipate these effects, alongside specific spatial behaviours
358 thought to drive social network position. This practice will help to buffer for the fact that the
359 spatial environment not only correlates with social proximity, but can alter the fabric of the
360 network itself.

The landscape of sociality

362 One of the foremost advantages of our approach is the ability to flexibly investigate two-
363 dimensional spatial patterns of social network centrality. This allowed us to qualitatively
364 assess the spatial structure of the social network, while providing clues towards the causal
365 factors. Most notably, betweenness peaked in the north-northeast of the system, likely
366 because the far northeastern community is relatively isolated from the rest of the population
367 due to the landscape structure (Figure 2), so that many 'social paths' that traverse the
368 population (the criteria for betweenness centrality) go through individuals in this intermediate
369 (north-northeast) area. That is, individuals living in this area are more likely to be connected
370 to both the far eastern communities and the central and western ones.

371 As expected, direct centrality metrics (group size, degree, and strength) were affected by
372 local population density, which peaks in the central north study area due to the concentration
373 of high quality grazing (Clutton-Brock *et al.* 1982). Individuals' resource selection behaviours
374 increase local density in this area (Clutton-Brock *et al.* 1982; Mcloughlin *et al.* 2006), and will
375 increase social connectivity as a result (Ostfeld *et al.* 1986; Sanchez & Hudgens 2015;
376 Webber & Vander Wal 2018). This comprises strong evidence for density-related increases
377 in social contact frequency, and accentuates the vital importance of considering resource
378 distribution, habitat selection, and population structure when examining social network
379 correlates (Spiegel *et al.* 2016; Webber & Vander Wal 2018; Farine & Sheldon 2019; He *et*
380 *al.* 2019). However, because density was accounted for as a fixed effect in the models, the
381 spatial patterns of location effects for the direct metrics did not strictly follow the spatial
382 pattern of density. Instead, these metrics peaked in the centre of the study population,
383 demonstrating that individuals living in this central region are more well-connected *when*
384 *accounting for population density*, and could represent a difficult-to-detect spatial
385 observation bias or an edge effect where social pairs are less likely to occur at the fringes of
386 the study system. Combining these spatial components allowed us to effectively differentiate

387   what we do know (that greater population density drives increased social connectedness)
388   from what we do not (the drivers of greater sociality for individuals in the central area).

389   Without using the SPDE effect (i.e., relying only on generalised pairwise space sharing
390   rather than accounting for specific two-dimensional spatial patterns), these insights into
391   these patterns may have been harder to detect. An alternative method could involve splitting
392   the population into subpopulations and analysing them separately or comparing them, but
393   this method has been shown to be less powerful in this population (Albery *et al.* 2019), and
394   is ultimately based on arbitrary choices if a population is mixed. The causes of the spatial
395   distribution of clustering remain unresolved, but the pattern highlights areas where
396   individuals are connected together in triads or tight cliques, and appears to be negatively
397   correlated with betweenness (Figure 4). For traits such as this, it is unlikely that a simpler
398   explanatory variable could be formulated to quantify the spatial-social processes at play.

399   Regardless of the causes of the spatial patterns, such fine-scale variation across the
400   landscape holds important ecological consequences, particularly for the more complex
401   network metrics. For instance, the areas of high clustering may act as 'incubator' areas
402   where cliques can develop new socially influenced behaviours (Centola 2018; Guilbeault *et*
403   *al.* 2018; Firth 2020). The high contact rates in the northern central areas might sustain high
404   local burdens of directly transmitted diseases (Cote & Poulin 1995), while individuals
405   inhabiting the high-betweenness intermediate areas may be important for transmitting novel
406   diseases across the population as a whole (VanderWaal *et al.* 2014).

Analytical benefits of INLA animal models

408   Analyses using multiple layers of different behaviours are well-suited to extricating space
409   and sociality in wild animal systems (Silk *et al.* 2018; Webber & Vander Wal 2018; Finn *et al.*
410   2019), and there is increasing conceptual and analytical overlap with the related field of
411   movement ecology (Jacoby & Freeman 2016; Mourier *et al.* 2019; Pasquaretta *et al.* 2020).
412   Notably, many spatial-social studies suffer from the necessity to reduce complex movement
413   patterns into simpler metrics, which risks losing important information in the process. As
414   such, recent studies have pushed for researchers to incorporate movement trajectories
415   themselves into complex network data structures (Mourier *et al.* 2019). Our approach allows
416   incorporation of multiple dyadic and non-dyadic behavioural measures, and with several
417   analytical timescales, offering an alternative workaround to this problem. Although other
418   methods can control for point locations (e.g. using autoregressive processes and
419   row/column effects; Stopher *et al.* 2012b), INLA models allow greater precision, fit quickly,
420   and allow incorporation of spatiotemporal structuring. Furthermore, plotting the SPDE effect
421   in two dimensions, as in Figure 4, gives an easily interpretable and intuitive portrayal of

422   network traits in space that can be hard to visualise using other methods. For these reasons,

423   we highly recommend further exploration of INLA animal models as a flexible method with

424   which to extricate individual, demographic, spatial, and temporal contributors to sociality

425   where sample sizes are sufficient (Thomson *et al.* 2018; Webber & Vander Wal 2018). In

426   addition to carrying out network-level manipulations (Daraganova *et al.* 2012; Davis *et al.*

427   2015; Firth & Sheldon 2016; Farine 2017), researchers concerned about spatial confounding

428   could implement relatively familiar linear models of social behaviour, but with additional

429   spatial components such as SPDE random effects and similarity matrix variance

430   components, with trustworthy and interpretable results (Albery *et al.* 2020a).

Non-spatial drivers of social network positioning

432   Although space accounted for an overwhelming amount of variation, many non-spatial

433   factors had substantial effects. The random effect for interannual variation was substantial,

434   and there were detectable linear annual effects and population size effects, as expected

435   given the important roles of demography in structuring social networks (Shizuka & Johnson

436   2019). Interestingly, there was a substantial positive association with study year that was not

437   attributable to the growth in population size over the same period. It is possible that this

438   represents a change in the deer's social phenotypes over time, although the potential

439   mechanisms would benefit from further examination. Individual-level factors had weaker

440   contributions to model fit and smaller effect sizes: most notably, genetic and individual

441   random effects were negligible when spatial autocorrelation was accounted for, confirming

442   the importance of considering space when assessing heritability independently of space in

443   this population (Stopher *et al.* 2012a). Nevertheless, individual-level effects were

444   encouragingly still detectable and significant, particularly for simpler "direct" metrics. It is

445   possible that more complex social network positions are less determined by individual social

446   behaviours, particularly for animals with fission-fusion societies such as the deer; this

447   hypothesis could be tested using similar spatial-social analyses in a number of other

448   systems. This finding demonstrates that even when spatial structuring plays a vital role in

449   determining social network structure, controlling for this structuring analytically can reveal

450   important, conservative individual-level effects. Future analyses within this population, and

451   potentially other long-term studies, could take advantage of this framework by including

452   environmental drivers such as food availability and climatic factors to explain patterns of

453   social connectivity, while further unpicking the causes of the individual-level trends that we

454   observed.

455   Our revelation that sociality covaries predictably with a suite of different spatial behaviours

456   contributes to a rapidly growing literature connecting elements of the external environment,

457   intrinsic phenotypes, spatial behaviours, and social network structure in wild animals. By

458   employing similar approaches, we hope that future investigations in this and other ecological

459   systems will be able to more easily identify, interrogate, and deconstruct the interplay

460   between multiple spatial and social behaviours. As well as increasing the robustness of such

461   studies to spatial confounding, the multivariate nature of these analyses will help to open up

462   new and exciting avenues for investigating the spatial-social interface in ecology.

463

464
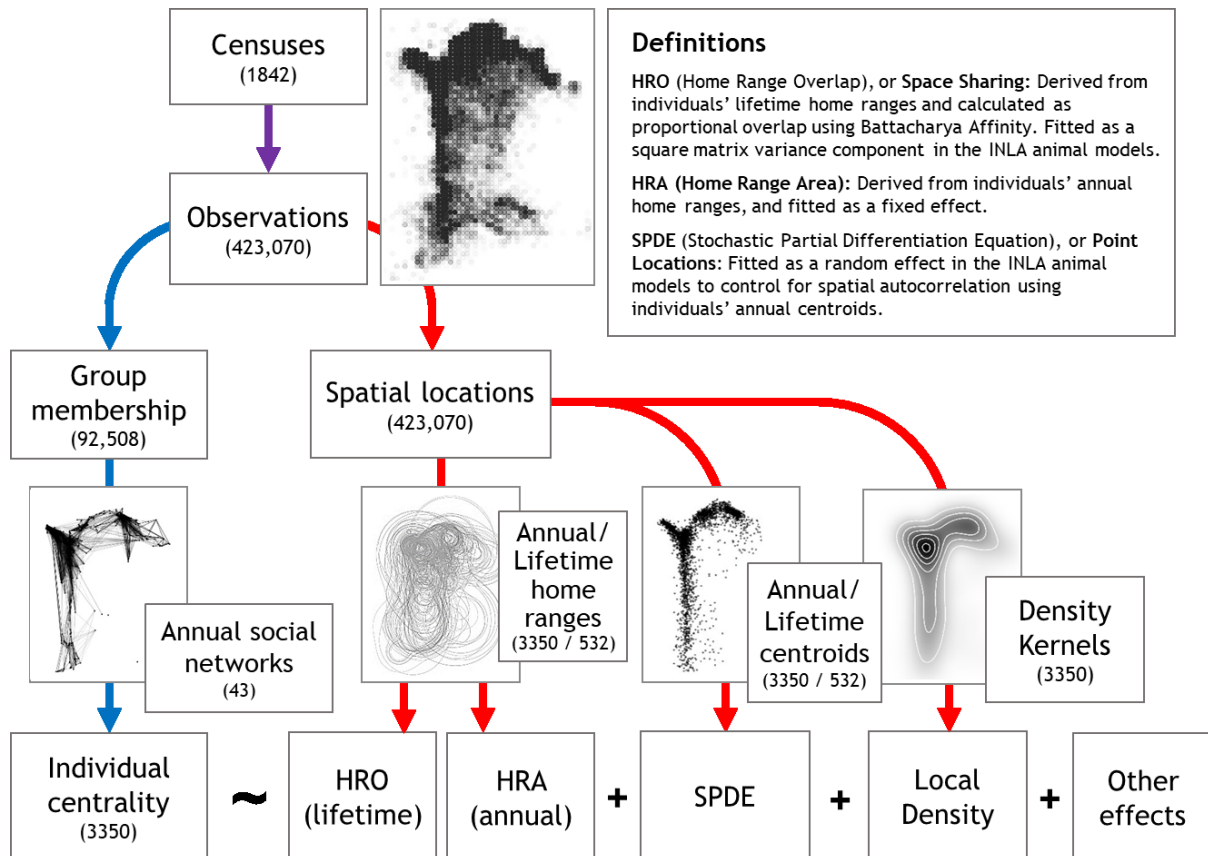
465
466   Figure 1: Data processing and analysis pipeline, demonstrating how behavioural census
467   data were collected, used to derive social and spatial behavioural traits, and fitted in INLA
468   animal model GLMMs. Numbers in brackets represent sample sizes, and only include
469   females aged 3+ years. Blue arrows represent social behaviour; red arrows represent spatial
470   behaviours. See methods for the fixed and random effects. The text box displays the
471   definitions for the different spatial effects.

472
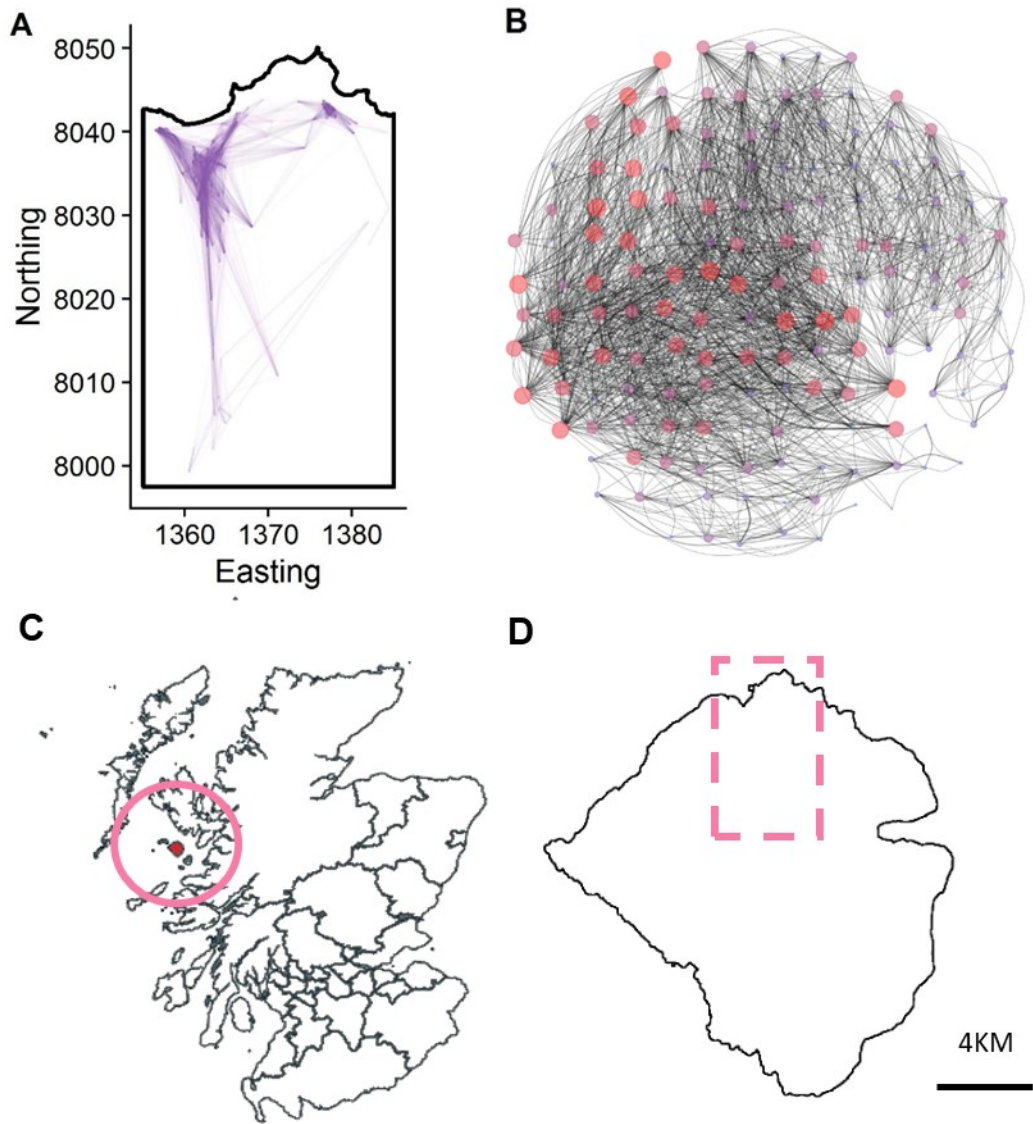
Figure 2: Spatial structuring of the 2016 social association network as a representative example. A: the spatial locations (centroids) of individual deer, connected by their social associations. Line opacity and width are weighted by connection strength. Ten axis units = 1KM. B: the same social network with the nodes positioned in a network spring-layout (Csardi & Nepusz 2006) and then expanded into an even, circular grid according to their nearest spatial positions in A. The points' (i.e. nodes') sizes and colours show individuals' strength centrality (large and red=high strength; small and blue=low strength). Thickness of the lines (i.e. edges) connecting them shows dyadic association strength between individuals. C: the position of the Isle of Rum in Scotland and D: the position of the examined area in the context of the Island as a whole.

483
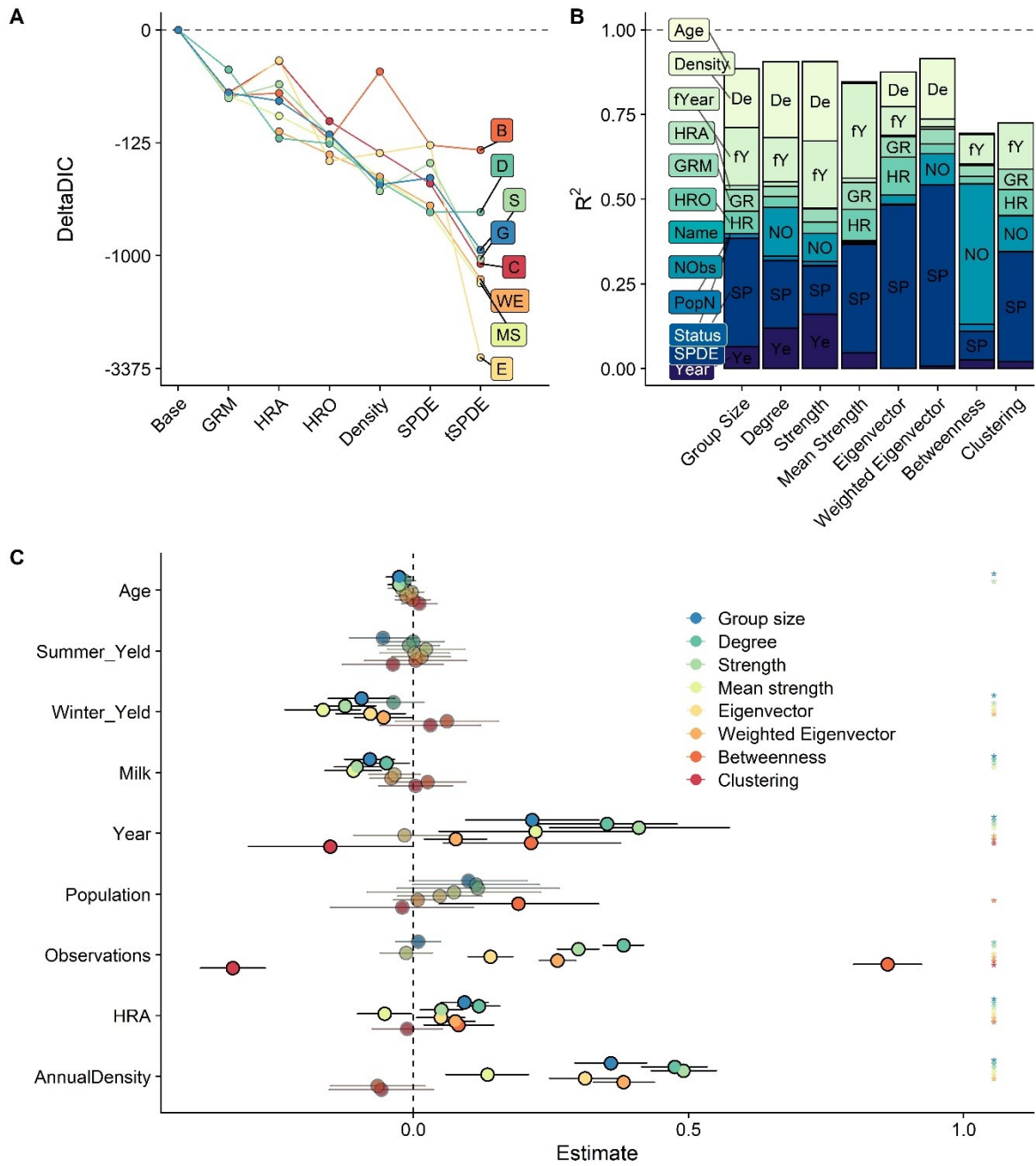
484
485 Figure 3: Model outputs demonstrating strong effects of spatial and non-spatial drivers on
486 social network positions. A: DIC changes associated with addition of different spatial
487 components, for all eight social network centrality measures. Variables are arranged in order
488 of mean contribution to model fit, which varied little among response variables. Different
489 colours correspond to different network centrality response variables, with the same colour
490 key as panel C. GRM = Genomic Relatedness Matrix. HRA = Home Range Area. HRO =
491 home range overlap. The SPDE models are differentiated into those using annual centroids
492 ("SPDE") and the version with spatiotemporally varying annual spatial fields ("tSPDE"). B:
493 Variance accounted for by each variable for all eight network position measures, expressed
494 as contribution to R^2 in the annual model (squared correlation between observed and
495 predicted values). Different shades correspond to different variables. fYear = year as a
496 categorical random effect. HRA = Home Range Area. GRM = Genomic Relatedness Matrix.
497 HRO = home range overlap. Name = individual identity. NObs = number of observations
498 (i.e., sampling bias). PopN = population size. Status = reproductive status. SPDE = point
499 location effects estimated using the Stochastic Partial Differentiation Equation effect in the

INLA models. For all response variables, individual level effects (Age, Reproductive Status, Name) had a negligible effect. C: Fixed effect estimates for the models. Fixed effects are grouped into individual factors (age and three reproductive status effects), annual factors (continuous time in years since study began, and annual population size), and sampling factors (observation number). Reproductive status effects are separated into four levels: did not reproduce (the intercept); calf died in the first few months of life ("Summer Yeld"); calf died during the winter ("Winter Yeld"); and calf survived to May the following year ("Milk"). Different colours correspond to different network centrality response variables. Points represent the posterior mean; error bars denote the 95% credibility intervals for the effects. Asterisks denote significant variables (i.e., those whose estimates did not overlap with zero). Significant variables are fully opaque, while non-significant ones are transparent.
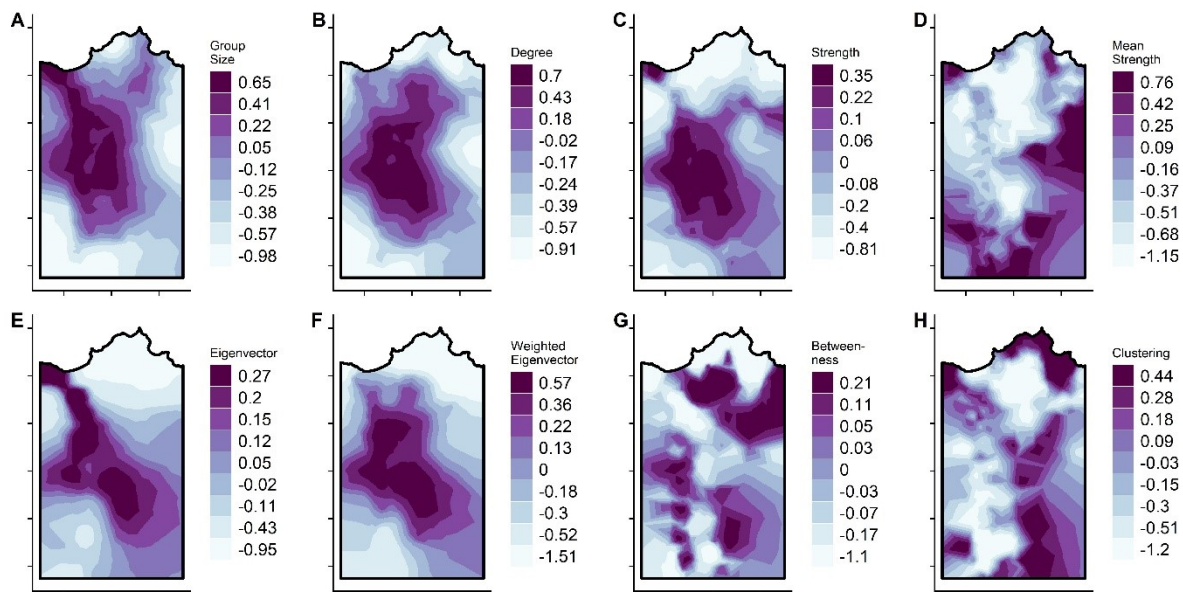
Figure 4: Spatial fields for the SPDE random effect for each response variable, taken from the INLA animal models and based on annual centroid point locations. Metrics can be conceptualised as simpler "direct" metrics (top row) and more complex "indirect" metrics (bottom row). Darker colours correspond to greater values. Each axis tick corresponds to 1km; for the values associated with the Easting and Northings, see Figure 1.

Acknowledgements

References

532   Albery, G.F., Becker, D.J., Kenyon, F., Nussey, D.H. & Pemberton, J.M. (2019). The fine-
533   scale landscape of immunity and parasitism in a wild ungulate population. *Integr.*
534   *Comp. Biol.*, icz016, 1–11.

535   Albery, G.F., Kirkpatrick, L., Firth, J.A. & Bansal, S. (2020a). Unifying spatial and social
536   network analysis in disease ecology. *J. Anim. Ecol.*, 1–17.

537   Albery, G.F., Newman, C., Ross, J.B.G.B., Macdonald, D.W., Bansal, S., Buesching, C.D., *et*
538   *al.* (2020b). Negative density-dependent parasitism in a group-living carnivore. *Proc. R.*
539   *Soc. B Biol. Sci.*, 287, 20202655.

540   Albery, G.F., Watt, K.A., Keith, R., Morris, S., Morris, A., Kenyon, F., *et al.* (2020c).
541   Reproduction has different costs for immunity and parasitism in a wild mammal. *Funct.*
542   *Ecol.*, 34, 229–239.

543   Brent, L.J.N. (2015). Friends of friends: Are indirect connections in social networks important
544   to animal behaviour? *Anim. Behav.*, 103, 211–222.

545   Cairns, S.J. & Schwager, S.J. (1987). A comparison of association indices. *Anim. Behav.*,
546   35, 1454–1469.

547   Calenge, C. (2011). *Home range estimation in R: the adehabitatHR package*. Available at:
548   https://cran.r-project.org/web/packages/adehabitatHR/index.html. Last accessed 10
549   March 2020.

550   Castles, M., Heinsohn, R., Marshall, H.H., Lee, A.E.G., Cowlishaw, G. & Carter, A.J. (2014).
551   Social networks created with different techniques are not comparable. *Anim. Behav.*,
552   96, 59–67.

553   Centola, D. (2018). *How Behavior Spreads: The Science of Complex Contagions*. Princeton
554   Analytical Sociology Series.

555   Clutton-Brock, T.H., Albon, S.D. & Guinness, F.E. (1989). Fitness costs of gestation and
556   lactation in wild mammals. *Nature*, 337, 260–262.

557   Clutton-Brock, T.H., Guinness, F.E. & Albon, S.D. (1982). *Red Deer: Behavior and Ecology*
558   *of Two Sexes*. University of Chicago Press, Chicago, IL.

559   Cote, I.M. & Poulin, R. (1995). Parasitism and group size in social animals: A meta-analysis.

Behav. Ecol., 6, 159–165.

Croft, D.P., James, R. & Krause, J. (2008). *Exploring animal social networks*. Princeton University Press.

Csardi, G. & Nepusz, T. (2006). The igraph software package for complex network research. *InterJournal Complex Syst.*, Complex Sy, 1695.

Daraganova, G., Pattison, P., Koskinen, J., Mitchell, B., Bill, A., Watts, M., *et al.* (2012). Networks and geography: Modelling community network structures as the outcome of both spatial and network processes. *Soc. Networks*, 34, 6–17.

Davis, S., Abbasi, B., Shah, S., Telfer, S. & Begon, M. (2015). Spatial analyses of wildlife contact networks. *J. R. Soc. Interface*, 12.

Farine, D.R. (2017). A guide to null models for animal social network analysis. *Methods Ecol. Evol.*, 8, 1309–1320.

Farine, D.R. & Sheldon, B.C. (2019). Stable multi-level social structure is maintained by habitat geometry in a wild bird population. *bioRxiv*, 1–30.

Finn, K.R., Silk, M.J., Porter, M.A. & Pinter-Wollman, N. (2019). The use of multilayer network analysis across social scales in animal behaviour. *Anim. Behav.*, 149, 7–22.

Firth, J.A. (2020). Considering complexity: animal social networks and behavioural contagions. *Trends Ecol. Evol.*, 35, 100–104.

Firth, J.A., Cole, E.F., Ioannou, C.C., Quinn, J.L., Aplin, L.M., Culina, A., *et al.* (2018). Personality shapes pair bonding in a wild bird social system. *Nat. Ecol. Evol.*, 2, 1696–1699.

Firth, J.A. & Sheldon, B.C. (2016). Social carry-over effects underpin trans-seasonally linked structure in a wild bird population. *Ecol. Lett.*, 19, 1324–1332.

Firth, J.A., Voelkl, B., Crates, R.A., Aplin, L.M., Biro, D., Croft, D.P., *et al.* (2017). Wild birds respond to flockmate loss by increasing their social network associations to others. *Proc. R. Soc. B Biol. Sci.*, 284.

Franks, D.W., Ruxton, G.D. & James, R. (2010). Sampling animal association networks with the gambit of the group. *Behav. Ecol. Sociobiol.*, 64, 493–503.

Froy, H., Börger, L., Regan, C.E., Morris, A., Morris, S., Pilkington, J.G., *et al.* (2018). Declining home range area predicts reduced late-life survival in two wild ungulate populations. *Ecol. Lett.*, 21, 1001–1009.

591   Froy, H., Walling, C.A., Pemberton, J.M., Clutton-brock, T.H. & Kruuk, L.E.B. (2016).
592   Relative costs of offspring sex and offspring survival in a polygynous mammal. *Biol.*
593   *Lett.*, 12, 20160417.

594   Guilbeault, D., Becker, J. & Centola, D. (2018). Complex Contagions: A Decade in Review.
595   pp. 3–25.

596   He, P., Maldonado-chaparro, A.A. & Farine, D.R. (2019). The role of habitat configuration in
597   shaping social structure: a gap in studies of animal social complexity. *Behav. Ecol.*
598   *Sociobiol.*, 73.

599   Holand, A.M., Steinsland, I., Martino, S. & Jensen, H. (2013). Animal Models and Integrated
600   Nested Laplace Approximations. *Genes|Genomes|Genetics*, 3, 1241–1251.

601   Huisman, J., Kruuk, L.E.B., Ellis, P.A., Clutton-Brock, T.H. & Pemberton, J.M. (2016).
602   Inbreeding depression across the lifespan in a wild mammal population. *Proc. Natl.*
603   *Acad. Sci.*, 113, 201518046.

604   Jacoby, D.M.P. & Freeman, R. (2016). Emerging Network-Based Tools in Movement
605   Ecology. *Trends Ecol. Evol.*, 31, 301–314.

606   Krause, J., James, R., Franks, D.W. & Croft, D.P. (2015). *Animal social networks*. Oxford
607   University Press, Oxford, UK.

608   Kruuk, L.E.B. (2004). Estimating genetic parameters in natural populations using the "animal
609   model." *Philos. Trans. R. Soc. B Biol. Sci.*, 359, 873–890.

610   Lindgren, F. & Rue, H. (2015). Bayesian Spatial Modelling with R-INLA. *J. Stat. Softw.*, 63,
611   1–25.

612   Lindgren, F., Rue, H. & Lindstrom, J. (2011). An explicit link between Gaussian fields and
613   Gaussian Markov random fields: the stochastic partial differential equation approach. *J.*
614   *R. Stat. Soc. B*, 73, 423–498.

615   Mcloughlin, P.D., Boyce, M.S., Coulson, T. & Clutton-brock, T. (2006). Lifetime reproductive
616   success and density- dependent , multi-variable resource selection. *Proc. R. Soc. B*
617   *Biol. Sci.*, 1449–1454.

618   Mourier, J., Lédée, E.J.I. & Jacoby, D.M.P. (2019). A multilayer perspective for inferring
619   spatial and social functioning in animal movement networks. *bioRxiv*.

620   Ostfeld, R.S., Lidicker, W.Z., Heske, E.J., Ostfeld, R.S., Lidicker, W.Z. & Heske, E.J. (1986).
621   The Relationship between Habitat Heterogeneity, Space Use, and Demography in a
622   Population of California Voles. *J. Mammal.*, 45, 433–442.

623   Pasquaretta, C., Dubois, T., Gomez-Moracho, T., Perilhon Delepoulle, V., Le Loc'h, G.,
624   Heeb, P., *et al.* (2020). Analysis of temporal patterns in animal movement networks.
625   *Methods Ecol. Evol.*, 0–1.

626   Pinter-Wollman, N., Hobson, E.A., Smith, J.E., Edelman, A.J., Shizuka, D., De Silva, S., *et*
627   *al.* (2014). The dynamics of animal social networks: Analytical, conceptual, and
628   theoretical advances. *Behav. Ecol.*, 25, 242–255.

629   Regan, C.E., Pilkington, J.G., Berenos, C., Pemberton, J.M., Smiseth, P.T. & Wilson, A.J.
630   (2016). Accounting for female space sharing in St. Kilda Soay sheep (Ovis aries)
631   results in little change in heritability estimates. *J. Evol. Biol.*, 30, 96–111.

632   Robert, K., Garant, D. & Pelletier, F. (2012). Keep in touch: Does spatial overlap correlate
633   with contact rate frequency? *J. Wildl. Manage.*, 76, 1670–1675.

634   Sah, P., Mann, J. & Bansal, S. (2018). Disease implications of animal social network
635   structure: A synthesis across social systems. *J. Anim. Ecol.*, 87, 546–558.

636   Sanchez, J.N. & Hudgens, B.R. (2015). Interactions between density, home range
637   behaviors, and contact rates in the Channel Island fox (*Urocyon littoralis*). *Ecol. Evol.*,
638   5, 2466–2477.

639   Shizuka, D. & Johnson, A.E. (2019). How demographic processes shape animal social
640   networks. *Behav. Ecol.*, 1–11.

641   Silk, M.J., Finn, K.R., Porter, M.A. & Pinter-Wollman, N. (2018). Can Multilayer Networks
642   Advance Animal Behavior Research? *Trends Ecol. Evol.*, 33, 376–378.

643   Silk, M.J., Hodgson, D., Rozins, C., Croft, D., Delahay, R., Boots, M., *et al.* (2019).
644   Integrating social behaviour, demography and disease dynamics in network models:
645   applications to disease management in declining wildlife populations. *Philos. Trans. R.*
646   *Soc. B*, 374, 20180211.

647   Sosa, S., Sueur, C. & Puga-Gonzalez, I. (2020). Network measures in animal social network
648   analysis: their strengths, limits, interpretations and uses. *Methods Ecol. Evol.*

649   Spiegel, O., Leu, S.T., Sih, A. & Bull, C.M. (2016). Socially interacting or indifferent
650   neighbours ? Randomization of movement paths to tease apart social preference and
651   spatial constraints. *Methods Ecol. Evol.*, 971–979.

652   Spiegel, O., Sih, A., Leu, S.T. & Bull, C.M. (2018). Where should we meet? Mapping social
653   network interactions of sleepy lizards shows sex-dependent social network structure.
654   *Anim. Behav.*, 136, 207–215.

655   Stopher, K. V., Nussey, D.H., Guinness, F., Morris, A., Pemberton, J.M., Clutton-Brock, T.H.,
656   *et al.* (2012a). Re-mating across years and intralineage polygyny are associated with
657   greater than expected levels of inbreeding in wild red deer. *J. Evol. Biol.*, 25, 2457–
658   2469.

659   Stopher, K. V, Walling, C. a, Morris, A., Guinness, F.E., Clutton-brock, T.H., Pemberton,
660   J.M., *et al.* (2012b). Shared spatial effects on quantitative genetic parameters:
661   accounting for spatial autocorrelation and home range overlap reduces estimates of
662   heritability in wild red deer. *Evolution*, 66, 2411–26.

663   Thomson, C.E., Winney, I.S., Salles, O.C. & Pujol, B. (2018). A guide to using a Multiple-
664   Matrix animal model to disentangle genetic and nongenetic causes of phenotypic
665   variance. *PLoS One*, 13, e0197720.

666   VanderWaal, K.L., Atwill, E.R., Isbell, L.A. & McCowan, B. (2014). Linking social and
667   pathogen transmission networks using microbial genetics in giraffe (Giraffa
668   camelopardalis). *J. Anim. Ecol.*, 83, 406–414.

669   Vander Wal, E., Laforge, M.P. & McLoughlin, P.D. (2014). Density dependence in social
670   behaviour: Home range overlap and density interacts to affect conspecific encounter
671   rates in a gregarious ungulate. *Behav. Ecol. Sociobiol.*, 68, 383–390.

672   Webber, Q.M.R. & Vander Wal, E. (2018). An evolutionary framework outlining the
673   integration of individual social and spatial ecology. *J. Anim. Ecol.*, 87, 113–127.

674   Whitehead, H. (2008). *Analyzing animal societies : quantitative methods for vertebrate social*
675   *analysis*. University of Chicago Press.

676   Yang, J., Lee, S.H., Goddard, M.E. & Visscher, P.M. (2011). GCTA: A Tool for Genome-wide
677   Complex Trait Analysis. *Am. J. Hum. Genet.*, 88, 76.

678   Zuur, A.F., Ieno, E.N. & Saveliev, A.A. (2017). *Beginner's guide to spatial, temporal, and*
679   *spatial-temporal ecological data analysis with R-INLA*. Highstat Ltd.

680